Department of Pharmaceutical Technology, Faculty of Pharmacy, Complutense University, Madrid, Spain

Nystatin antifungal micellar systems on endotracheal tubes: development, characterization and *in vitro* evaluation

C. Benavent*, V. García-Herrero, C. Torrado, S. Torrado-Santiago

Received July 24, 2018, accepted November 10, 2018

**Corresponding author: Carlos Benavent, Department of Pharmaceutical Technology, Faculty of Pharmacy, Complutense University, Plaza Ramón y Cajal s/n, Madrid 28040, Spain*
carlosbenavent@ucm.es

Pharmazie 74: 34–38 (2019) *doi: 10.1691/ph.2019.8138*

Decontamination of patients' clinical devices in intensive care units is generally performed with an antifungal suspension. Nystatin is a widely-used high spectrum antifungal due to its low systemic absorption. However, nystatin has high hydrophobicity which hinders the contact with the internal lumen of the devices. In this work, hydrophilic micellar systems of nystatin were developed with sodium deoxycholate on silicone endotracheal tubes. The physical characteristics of the micellar system at different nystatin:deoxycholate ratios were studied using scanning electron microscopy, X-ray powder diffraction and differential scanning calorimetry. The electron microscopy results reveal that the deoxycholate micellar system altered the surface morphology, and the size of the aggregates was observed to be smaller. The hydrophilic structures of deoxycholate produce systems with a high surface area containing nystatin molecules on their interior. The X-ray and differential scanning calorimetry assays revealed a typical change in the crystallinity of micellar systems when the deoxycholate proportion increases. The endothermic peak of nystatin was not observed in the micellar systems as a consequence of the reduced crystallinity. Nystatin was homogenously dispersed in the surfactant matrix. Micellar systems with 1:0.8 nystatin:deoxycholate ratio (MS-N:DC [1:0.8]) showed increased antifungal activity compared to nystatin raw material. Micellar systems also achieved an over 40% inhibition of *Candida albicans* biofilm formation. The results obtained in this study conclude that the higher hydrophilic characteristic of the surfactant deoxycholate enhances nystatin penetration into the surface of the endotracheal tubes.

1. Introduction

Fungal infections by Candida species, mainly *C. albicans*, are considered a major public health issue (Ng et al. 2015). *C. albicans* biofilm formation (Uppuluri et al. 2009) on clinical devices enhances its pathogenic capacity, as it increases resistance to immune-mediated defences (Mayer et al. 2013) and reduces susceptibility to antifungal drugs (Tobudic et al. 2012; Desai and Mitchell 2015). Despite the dominance of *C. albicans*, other emergent species associated to biofilm formation should also be considered (Leite de Andrade et al. 2017; Marcos-Zambrano et al. 2017; Paredes et al. 2015).

Patients in intensive care units are generally treated with antifungal suspensions to ensure the decontamination of the devices. The accurate detection of contaminated devices (Martin-Rabadán et al. 2017) is an essential factor for guaranteeing effective treatment. Several drugs have been described as potentially useful for preventing *C. albicans* biofilm formation (Yuang et al. 2012; Chandra and Ghanoum 2017), even against resistant strains (Melkusová et al. 2004).

An anti-biofilm effect using surfactants in chlorhexidine micellar systems resulted in the enhanced wettability of the silicone surface of the material, which reduces biofilm formation for a longer period compared with chlorhexidine raw material (Tambunlertchai et al. 2017). Several micellar systems with hydrophilic carriers have also demonstrated an increased anti-biofilm and antifungal effect (Abu Hashim et al. 2015). Surfactants such as sodium dodecyl sulphate and cremophor show an anionic behaviour which promotes absorption in the membranes and enhances its antibiotic or antifungal action from inside the micellar system (Li et al. 2010). Amphotericin B (AmB) was commercialized as a dimeric form in a micellar system of sodium deoxycholate (DC), but showed toxicity (Gangadhar et al. 2014). New formulations such as lipid micellar systems and liposomes have subsequently been developed (López-Sánchez et al. 2018). Nystatin (Nyst) has the advantage of being a spread spectrum antifungal that is easily accessible by hospital pharmacy services and has very few toxic effects due to the lack of systemic absorption. Nyst's high hydrophobic features imply less contact with the internal surface of silicone devices.

This work studies the formulation and characterization of Nyst micellar systems with DC. The effect of micellar systems on Nyst crystallinity, wettability and aqueous solubility was assessed using scanning electron microscopy (SEM), X-ray powder diffraction (XRPD) and diffraction scanning calorimetry (DSC) techniques. *In vitro* assays were done on silicone clinical devices to assess the antifungal and anti-biofilm effect of these micellar systems.

2. Investigations, research and discussion

2.1. Preparation of formulations

Aqueous suspension: a yellow coloured suspension was obtained. Nyst raw material precipitates rapidly and accumulates at the bottom of the tubes. Precipitated Nyst could be easily resuspended by manual agitation.

Physical mixture: the mixture of Nyst and DC produced a light yellow powder which occupied a greater volume than the Nyst raw material. The physical mixture remains in suspension for longer: the first precipitations did not appear until 10 min after being suspended.

Micellar system: the solubility of slightly water-soluble drugs can be increased through the addition of surfactants (Rangel-Yagui et al. 2005); we therefore designed a micellar system with DC as an anionic surfactant. This natural surfactant obtained from bile

acids can form micelles with low water-soluble compounds such as amphotericin B (Gangadhar et al. 2014). This system had the highest volume of all formulations, which may be due to its low apparent density. These properties resulted in a more homogeneous suspension that remained stable for longer, thus offering a more precise posology and easier dispersion throughout the oral cavity.

2.2. Scanning electron microscopy (SEM): morphology, size and shape characterization

Figure 1 shows the microphotographs of pure Nyst, DC raw material, PM-N:DC [1:0.8] and micellar systems: MS-N:DC [1:0.4] and MS-N:DC [1:0.8]. Pure nystatin (Fig. 1a) appears as aggregated polyhedral crystals with sharp and acicular forms of different sizes, from 2 to 5 µm. DC crystals (Fig. 1b) appear as scales with sizes ranging from 3 to 10 µm, presenting a larger flat area. Both components can be differentiated on PM-N:DC (1:0.8) (Fig. 1C). This sample shows larger aggregated crystals (10 µm) where DC scales can be observed with Nyst crystals on the surface. The DC crystals reveal changes in their appearance. For MS, the acicular particles of Nyst were not visible, which could be due to a change in hydrophilic characteristics which alters the morphology of the Nyst crystals during the drying process. MS-N:DC [1:0.4] (Fig. 1D) showed the evolution of DC crystals to smaller and more regular particles (1-2 µm), easily differentiated from the primary large scales of DC. These reduced particles are therefore likely to contain Nyst crystals (Palmeiro-Róldan et al. 2014). This process produces a larger surface area. An increase in the proportion of DC in MS-N:DC [1:0.8] led to larger regular DC particles (4-6 µm), and consequently enhanced the dissolution surface of Nyst (microphotograph not shown). This improvement may be due to the drying process of DC. Our results indicate that Nyst was homogenously dispersed in the surfactant matrix, as no Nyst crystals were observed. Similar results have been found for MS formation with a similar dissolution and drying technique (Fonseca-Berzal et al. 2015; Leonardi and Salomon 2013).

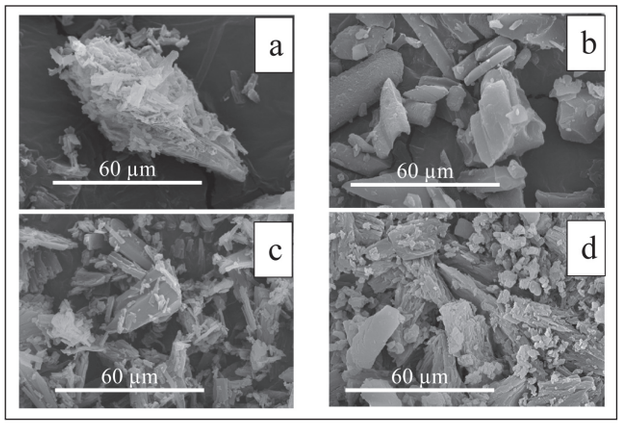

Fig. 1: SEM microphotographs of Nystatin raw material (a), sodium deoxycholate raw material (b), PM-N:DC 1:0.8 (c) and MS-N:DC 1:0.8 (d). Photographs magnification is 3000x.

2.3. Differential scanning calorimetry (DSC)

Figure 2 shows the DSC curve of pure Nyst, DC raw material, physical mixture 1:0.8 (w/w) (PM- N:DC [1:0,8]) and micellar systems with 1:0.4 (w/w) and 1:0.8 (w/w) ratios (MS-N:DC [1:0.4]; MS-N:DC [1:0.8]).

Nyst (Fig 2A) showed two endothermic peaks at 167.1 and 170.65 ºC, with enthalpy values of -20.22 and -61.38 (J/g) respectively. The largest endothermic peak at 170.65 ºC is characteristic of crystalline compounds, as has been previously described (Girotra et al. 2017). DC shows two endothermic peaks at 127.54 and 149.15 ºC (Fig. 2 B) with enthalpy values of -22.54 and -57.02 (J/g), which may be due to greater disorder in the crystallinity of DC (Palmeiro-Roldán et al. 2014; Vadlapatla et al. 2009).

PM-N:DcH 1:0.8 had an endothermic peak at 157.90 ºC (Fig. 1C), indicating an interaction between Nyst and DC, a lower Nyst fusion point and a higher fusion temperature in the main peak of DC. Similar patterns on fusion points have been described with mixtures of DC and benznidazole (Palmeiro-Roldán et al. 2014).

MS-N:DC [1:0.4] and MS-N:DC [1:0.8] show endothermic peaks at 142.03 ºC and 163.46 ºC (Figs. 2D and 2E). DSC patterns changed with the formation of micellar systems, as new endothermic peaks appeared. These peaks revealed a higher fusion point when the DC proportion was increased. The endothermic peak of Nyst was not observed on micellar systems, and a reduction in crystallinity was found when the DC proportion increased. The presence of amorphous forms may explain the reduced crystallinity observed in micellar systems (Talukder et al. 2011).

2.4. X-ray powder diffraction: size and structure characterization

Figure 3 shows the XRPD patterns of pure Nyst, raw DC, physical mixture PM-N:DC [1:0.8] and micellar systems 1:0 (w/w) (MS-N:DC [1:0]), 1:0.4 (w/w) (MS-N:DC [1:0.4]), and 1:0.8(w/w) (MS-N:DC [1:0.8]). DC (Fig 3A) presents several intense peaks at 13.02º, 14.14º, 15.94º and 19.26º 2θ for this crystalline surfactant with low molecular weight (Palmeiro-Roldán et al. 2014). Nyst raw material (Fig. 3B) shows a typically crystalline pattern with peaks at 8º, 14º, 16.5º and 20.5º 2θ (Park et al., 2015). As expected, the physical mixture of surfactant and drug, PM-N:DC [1:0.8] (Fig. 3C), led to a reduction in the intensity of the peaks of both components, with the appearance of one peak at 20.5º, related to nystatin. This may be explained by the dilution effect of the mixture (Cerdeira et al. 2013).

The MS-N:DC [1:0.4] diffractogram showed a significant decrease in intensity in the peaks for both substances, Nyst and DC (Fig. 3D), which is correlated with the SEM results. Nevertheless, the presence of intensity at 14º and 20.5º 2θ may indicate that some nystatin remains in a crystalline state in the micellar system (Vippagunta et al. 2002). A significant result in regard to diffraction peaks is the disappearance of DC peaks on MS-N:DC [1:0.8] after the dissolution and drying process (Fig. 3E). The pattern appears as a low crystallinity substance which correlates with the changes in shape and size observed in the SEM samples. This result is linked with the reduced crystallinity in recrystallized DC samples (result not shown). These reductions are frequently observed after the freeze-drying process or after other dissolution and vacuum drying processes (Leonardi et al. 2007; García-Herrero et al. 2017).

2.5. In vitro assay: antifungal activity

The *in-vitro* experimental study of antifungal activity was performed using the widely known and useful disc diffusion and agar dilution methods (Jorgensen et al. 1999). An aqueous solution of sodium deoxycholate was prepared as a negative control. The inhibition area was measured using a precision vernier caliper. All measurements were repeated three times and mean±SD was used to describe the measurements.

The initial and most important step for bacterial infection is bacterial adherence on surfaces. Table 1 shows the inhibition of fungal growth at 24 h and 72 h in an aqueous suspension of nystatin raw material compared to a micellar system (MS-N:DC [1:0.8]). The results show that control samples (uncoated silicone

Table 1: Inhibitory activities against *C. albicans* CECT 1394 by disc diffusion test

Sample	Growth inhibition area 24 h (mm)	Growth inhibition area 72 h (mm)
Blank	0.0 ± 0.00	0.0 ± 0.00
Control	0.0 ± 0.00	0.0 ± 0.00
Aqueous suspension	20.34 ± 0.42	18.64 ± 0.44
MS-N:DC [1:0.8]	22.83 ± 0.55	20.34 ± 0.82

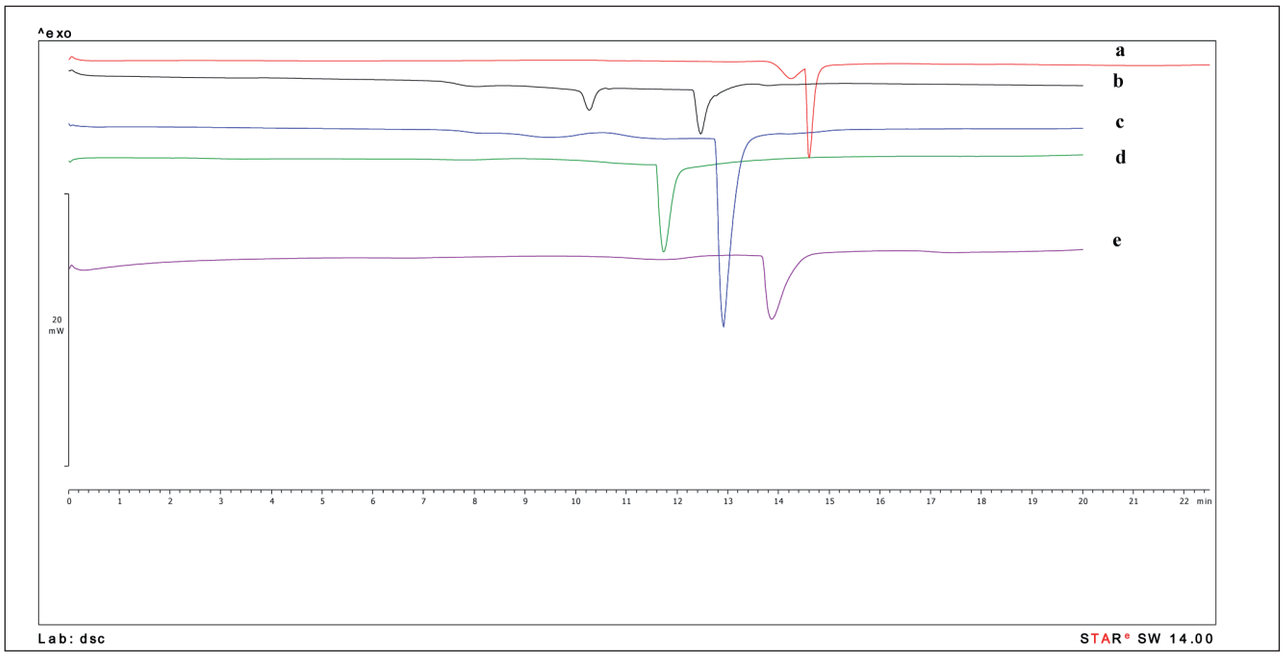

Fig. 2: DSC analysis. Pure nystatin (a), Sodium deoxycholate raw material (b), PM-N:DC 1:0.8 (w/w) (c), MS-N:DC 1:0.4 (w/w) (d) and MS-N:DC 1:0.8 (w/w) (e).

tubes) were rapidly contaminated by *C. albicans*, as they did not present an inhibition zone. Although the Nyst aqueous suspension had a large inhibition area (20.34±0.42 mm), the micellar system (MS-N:DC [1:0.8]) showed higher values for the inhibition area (22.83±0.55). These results can be explained by the arrangement of the hydrophilic groups of the surfactant (DC) on the surface of the Nyst particles, forming a micellar structure which minimizes the aggregation of particles and enhances the wettability of the silicone surface of a medical device (Jaiswal et al. 2015; Ansari et al. 2014). The greater antifungal activity of these systems may be due to the more hydrophilic character (El Shabouri 2002) of micelle structures with DC. The reduction in the aggregation of Nyst particles in micellar systems has been previously described in SEM assays. Thus MS-N:DC [1:0.8] coated silicone tubes were found to be capable of reducing the initial attachment of *C. albicans*. After 72 h, micellar formulations still maintained a greater inhibition area to *C. albicans* growth. These results indicate that silicone tubes coated with MS-N:DC [1:0.8] were effective in the long-term prevention

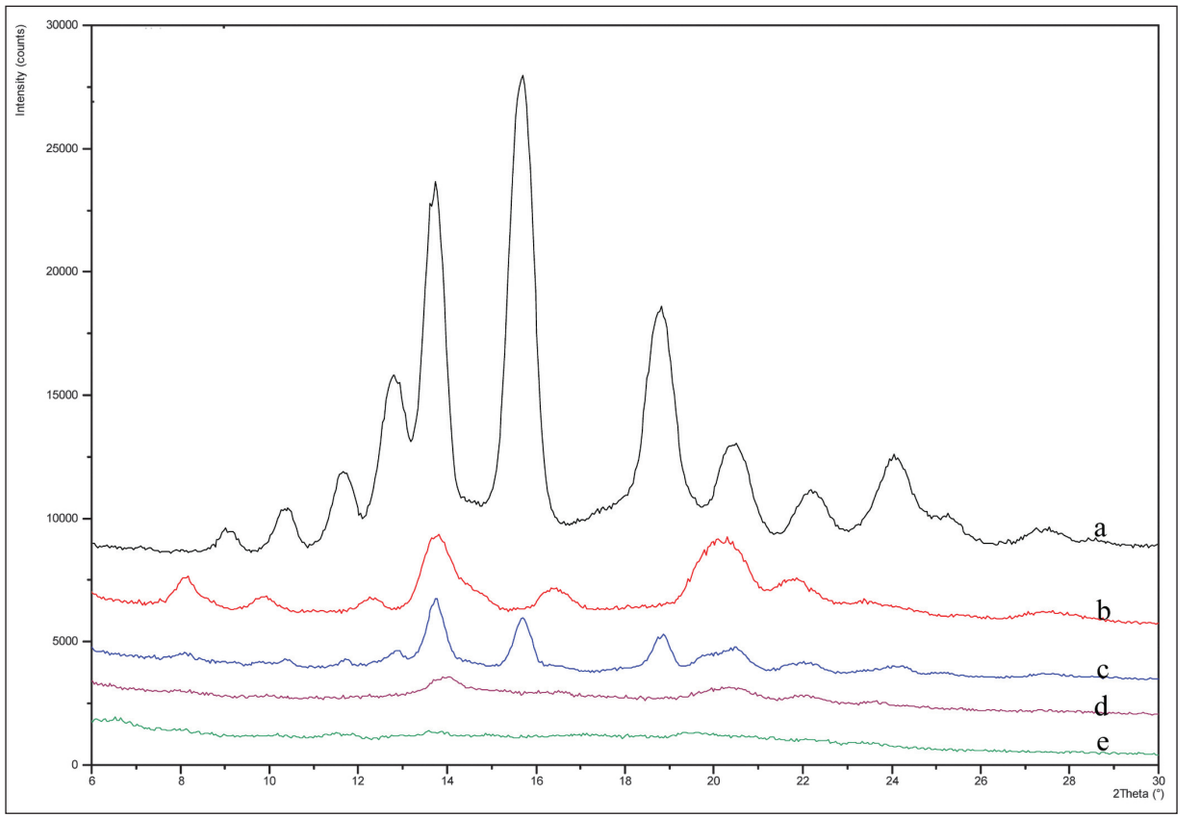

Fig. 3: X-Ray Powder Diffraction of: NaDcH raw material (a), pure Nyst (b), PM-N:DC 1:0.8 (c), MS-N:DC 1:0.4 (d) and MS-N:DC 1:0.8 (e).

of *C. albicans* contamination. X-ray characterization assays and the DSC analysis of Nyst micelles show an interaction between DC and Nyst crystalline morphology, which probably enhances its hydrophilic features and explains the increase in the inhibition zone. Similar results have been obtained with chlorhexidine micelles on silicone tubes (Tambunlertchai et al. 2017).

2.6. Biofilm formation and anti-biofilm activity

The results show that biofilm formation is completed within 48 h of harvesting, confirming the bibliographic data (Finkel and Mitchell 2011). Intermediate rinses were collected and harvested to assess the number of rinses required: the first rinse had uncountable colonies; the second rinse revealed a mean of 426.7±42.4 CFU/cm^2; the third, 102.2±3.15 CFU/cm^2; the fourth, 31.1±12.7 CFU/cm^2; and finally the fifth showed no colonies growing on the agar plate. After harvesting the pieces from the devices, the presence of biofilm was confirmed as *C. albicans* colonies growing on agar plates: 135.5 CFU±8.8 were counted. Previous assays have confirmed the need for suspensions with high Nyst concentrations to achieve preventive activity against biofilm formation (Dorocka-Bobkowska et al. 2003).

Table 2 shows all the results of the biofilm formation assay: drug-free controls showed the adherence capacity of *C. albicans* and

Table 2: Effect of nystatin formulations on *C. albicans* adherence and biofilm formation over a clinical material

	Candida albicans CETC 1394		
	Yeasts/cm^2 ± SD	Adherence (%)	p-value vs. control
Control	141.10 ± 11.7	100.0	---
Aqueous suspension	112.5 ± 10	79.7	p= 0.003
MS-N:DC (1:0.8)	82.20 ± 12	58.2	p= 0.0054

confirmed biofilm formation, as yeast cells were obtained in all plates; a mean number of 141.10±11.7 CFU/cm^2 yeast cells were counted. Blank plates showed no growth at all.

The administration of an aqueous suspension of Nyst led to the reduction of *C. albicans* adherence and the consequent biofilm formation in about 20% (see Table 2). This value is significantly different from the control (p=0.003). The crystalline structure of Nyst observed in the X-ray and DSC assays is probably related with high hydrophobic values, increasing the aggregation of particles. These characteristics and its low aqueous solubility reduce the antifungal activity of Nyst against biofilm formation. However, yeast adherence and biofilm formation was further inhibited in the presence of the Nyst micellar system (MS-N:DC [1:0.8]) by over 40 % (see Table 2). Consequently, the use of micellar systems with DC achieves a significant reduction (p=0.0054) in *C. albicans* biofilm formation compared to the Nyst suspension.

Nyst micellar systems with higher quantities of surfactant were associated with a greater interaction of Nyst with the hydrophilic structure of DC, as seen in the X-ray and DSC assays. The enhanced hydrophilic character of the surfactant enhances Nyst penetration in the surface of the clinical device. A similar interaction of Nyst with silicone surfaces was described in other Nyst micellar systems using Tween and Cremophor as surfactants (Li et al. 2010). The inhibition of biofilm formation was also obtained with other antifungal drugs when their hydrophilic features are enhanced (Jaiswal et al. 2015).

The results show that Nyst micellar systems with DC (MS-N:DC [1:0.8]) have significant preventive activity against biofilm formation. Further research may be required to assess new excipients with the potential to improve the contact of Nyst on the surface of clinical devices.

2.7. Conclusion

Formulating Nyst as a micellar system using DC as a surfactant considerably improves the management of this drug. A reduction in the aggregation of Nyst particles was observed in SEM assays. X-ray and DSC results showed a significant transformation from crystalline to amorphous forms when the DC proportion was increased. SEM images are correlated with DSC analysis, where a reduction in the degree of crystallinity of the formulation was observed.

The antifungal and antibiofilm activity seen in *in vitro* assays enhances the applicability of this new formulation. Additional parameters further complicate the situation encountered in clinical practice; however, a formulation offering preventive action with demonstrated antifungal activity is predicted to promote the appropriate treatment of oral candidiasis in critically ill patients and minimize the recontamination of biomedical devices. Further studies with the addition of hydrophilic carriers are required to increase adhesion and delay biofilm formation on endotracheal tubes.

3. Experimental

3.1. Materials and fungal strains

Nystatin (Nyst) (PubChem CID: 16219709) was supplied by Fragon (Tarrasa Spain), Sodium desoxycholate (DC) (PubChem CID: 91896239) was supplied by Fluka (Mexico, Mexico). *Candida albicans* strain (CECT1394) was a gift of Dr. Pérez Carrasco from Centro de Análisis Químico y Microbiológico (CAQYM), Universidad Alcalá de Henares (Madrid, Spain). Culture media were purchased from Pronadisa-Conda Lab (Madrid, Spain). All other chemicals were at least technical grade and were purchased from Merck (Madrid, Spain).

3.2. Preparation of formulations

Micellar systems contain proportions of Nyst and surfactant (DC) of 1:0.4 w/w (MS-N:DC [1:0.4]) and 1:0.8 w/w (MS-N:DC[1:0.8]). In these formulations, a solution was prepared by mixing different proportions of surfactant with an aqueous solution and adding the correct amount of Nyst, then shaking at 2000 rpm for 2 min. The micellar suspension formed was dried at 40 ºC during 24 h and sieved to achieve a particle size fraction of 1.2-0.1 mm. Finally, the vials were capped and stored at room temperature (22-24 ºC) in a desiccator containing silica gel. Recrystallized Nyst was obtained by the same method without the presence of surfactant.

The physical mixture (PM) was prepared by manually mixing the nystatin and DC in a ceramic bowl using a polymeric spatula. Formulations were prepared containing a similar proportion of drug:excipient (PM-N:DC [1:0.4] and PM-N:DC [1:0.8] w/w).

3.3. Scanning electron microscopy (SEM): morphology, size and shape characterization

Samples were mounted on double-faced adhesive tape and sputtered with a thin gold-palladium layer using a sputter coater (Emitech K550X). After coating, the samples were analysed with a Jeol JSM-6400® scanning electron microscope operated at an acceleration voltage of 20 kV. All micrographs were the product of secondary electron imaging used for surface morphology identification at magnifications of 1000x.

3.4. Differential scanning calorimetry (DSC)

DSC thermograms were obtained using an automatic thermal analyzer system (Mettler Toledo DSC 3, TA controller). Temperature calibration was performed using the Indium Calibration Reference Standard (transition point: 156.60 ºC). Samples were accurately weighed into aluminium pans, then hermetically sealed with aluminium lids and heated from 50 to 240 ºC at a heating rate of 10 ºC/min under constant purging of dry nitrogen at 20 ml/min. An empty pan, sealed in the same way as the sample, was used as a reference.

3.5. X-ray powder diffraction: structure and crystal size characterization

The XRPD patterns were recorded on an X-ray diffractometer (Philips X'Pert-MPD, CAI Difracción Rayos X, Farmacia, UCM). The samples were irradiated with monochromatized CuKα radiation (λ = 1.542 Å) and analysed between 5 and 50º (2θ). The 5-50 2è degree range was scanned at a step size of 0.04º and 1s per step in all cases, and the voltage and current used were 30 kV and 30 mA respectively.

3.6. In vitro assay: antifungal activity

The *in-vitro* experimental study of antifungal activity was performed using the widely known and useful disc diffusion and agar dilution methods (Jorgensen et al. 1999). An aqueous solution of DC was prepared as a negative control. Formulations were tested in a 15 mg/mL concentration. The inhibition area was measured using a precision vernier caliper. All measurements were repeated three times, and mean±SD was used to describe the measurements.

A quantity of agar was dissolved in water, and the solution was sterilized in autoclave at 1 atm pressure and 120 ºC during 60 min. The sterilized solution was cooled to room temperature and a specific volume of 0.5 McFarland standard diluted suspension of *C. albicans* was added before solidifying. In a sterile area under controlled conditions, a specific volume of the solution was spread over Petri dishes, avoiding the formation of bubbles and ensuring the entire dish was covered. The dishes were left in the sterile

area to cool completely and allow the gel to form. Once the gel had formed, the dishes were covered with parafilm and conserved under refrigeration for 24 h.
Sterilized diffusion discs of approximately 6 mm in diameter were loaded with 300 µl of each of the studied formulations. Each dish was fitted with a blank disc impregnated with respective solvents as a negative control. All plates were prepared in triplicate and incubated at 37 ºC for 24 h. At the end of the incubation, the diameter of the inhibition zone in each of the inoculated plates was measured with a precision Vernier caliper to evaluate the antifungal and antibacterial activity of all the formulations. Two measures were taken: 24 h and 72 h after harvesting.

3.7. Biofilm formation and anti-biofilm activity

The formation of fungal biofilm on the material surface was assessed using a method derived from Maki's classic technique (Maki et al. 1977), used to reveal catheter contamination in clinically used devices. Our technique simulates the colonization and consequent attachment of *C. albicans* in widely used clinical material. Briefly, 1 cm^2 of sterile silicone Mallinkroft tubes was cut in sterile conditions; a 36-h *C. albicans* culture was harvested on Mueller-Hinton agar and a fungal suspension was prepared in YPD liquid medium using a sterile swab containing 10^7 UFC/mL. The pieces were placed on sterile Petri dishes with 12 mL of fungal suspension during 48 h at 31.7 ºC. A set of reference dishes were also prepared. After harvesting, the pieces were rinsed five times with NaCl 9 $^0/_{00}$, allowing it to flow gently over the surface of the device to remove most of the planktonic organisms and ensure that the study was carried out on biofilm microorganisms.
After rinsing, the pieces were placed in 10 mL tubes with 3 mL of NaCl 9 $^0/_{00}$ and vortexed twice during 1 min at 1500 rpm; 50 mcl of this suspension was decimally diluted with NaCl 9 $^0/_{00}$ and harvested on Petri dishes with Sabouraud dextrose agar during 48 h at 31.7 ºC. After harvesting, the fungal colonies were counted.

3.8. In vitro assay: prevention of biofilm formation

The aim of this assay is to assess the activity of our experimental formulation in preventing biofilm formation. A 3-minute contact phase between the formulation and the non-contaminated devices took place before biofilm formation. This period simulates mouth-washing or rinsing with the formulation. The hypothetical preventive action would be detected in the case of any reduction in the UFC counted after harvesting.
An aqueous suspension of Nyst and a micellar system with a 1:0.8 (w/w) ratio of Nyst:DC was tested. The correct amount of each formulation powder was suspended in water.
Control Petri dishes, containing pieces of the device with no contact with the active formulations, were used to assess biofilm formation. Blank dishes were harvested as negative controls with non-contaminated solvents respectively.

3.9. Statistical methods

All microbiological assays were carried out on three samples with three replicates for each sample. The results were presented as mean±SD. The Mann-Whitney test was used for paired-group comparisons and p values of less than 0.05 were considered to indicate statistical significance (XLSTat Addinsoft, Barcelona Spain).

Acknowledgements: This research was funded by a grant from the Complutense University of Madrid and the Madrid Regional Government for the research group 910939.

Conflicts of interest: None declared.

References

Abu Hashim II, Ghazy NF, El-Shabouri MH (2015) Potential use of phospholipids in combination with hydrophilic carriers for enhancement of the dissolution and oral bioavailability of imidazole antifungal Class II drugs. Pharmazie 70: 706-715.
Ansari MA, Khan HM, Khan AA, Cameotra SS, Saquib Q, Musarrat J (2014) Gum arabic capped-silver nanoparticles inhibit biofilm formation by multi-drug resistant strains of Pseudomonas aeruginosa. J Basic Microbiol 54: 688-699.
Cerdeira AM, Mazzotti M, Gander B (2013) Formulation and drying of miconazole and itraconazole nanosuspensions. Int J Pharm 443: 209-220.
Chandra J, Ghannoum MA (2017) CD101, a novel echinocandin possesses potent anti-biofilm activity against early and mature *Candida albicans* biofilms. Antimicrob Agents Chemother 62: pii: e01750-17
Desai JV, Mitchell AP (2015) *Candida albicans* biofilm development and its genetic control. Microbiol Spectr 3(3): doi: 10.1128/microbiolspec.MB-0005-2014.
Dorocka-Bobkowska B, Konopka K, Düzgüneş N (2003) Influence of antifungal polyenes on the adhesion of *Candida albicans* and *Candida glabrata* to human epithelial cells in vitro. Arch Oral Biol 48: 805-814.
El-Shabouri MH (2002) Positively charged nanoparticles for improving the oral bioavailability of cyclosporin-A. Int J Pharm 249: 101-108.
Finkel JS, Mitchell AP (2011) Genetic control of *Candida albicans* biofilm development. Nat Rev Microbiol 9: 109-118.
Fonseca-Berzal C, Palmeiro-Roldán R, Escario JA, Torrado S, Arán VJ, Torrado-Santiago S, Gómez-Barrio A (2015) Novel solid dispersions of benznidazole: preparation, dissolution profile and biological evaluation as alternative antichagasic drug delivery system. Exp Parasitol 149: 84-91.
Gangadhar KN, Adhikari K, Srichana T (2014) Synthesis and evaluation of sodium deoxycholate sulfate as a lipid drug carrier to enhance the solubility, stability and safety of an amphotericin B inhalation formulation. Int J Pharm 471: 430-438.
García-Herrero V, Torrado C, García-Rodríguez JJ, López-Sánchez A, Torrado S, Torrado-Santiago S (2017) Improvement of the surface hydrophilic properties of naproxen particles with addition of hydroxypropylmethyl cellulose and sodium dodecyl sulphate: In vitro and in vivo studies. Int J Pharm 529: 381-390.
Girotra P, Thakur A, Kumar A, Singh SK (2017) Identification of multi-targeted anti-migraine potential of nystatin and development of its brain targeted chitosan nanoformulation. Int J Biol Macromol 96: 687-696.
Jaiswal S, Bhattacharya K, McHale P, Duffy B (2015) Dual effects of β-cyclodextrin-stabilised silver nanoparticles: enhanced biofilm inhibition and reduced cytotoxicity. J Mater Sci Mater Med 26: 5367.
Jorgensen JH, Turnidge JD, Washington JA (1999) Antibacterial susceptibility tests: dilution and disk diffusion methods. In Murray PR, Baron EJ, Pfaller MA, Tenover FC, Yolken RH (eds) Manual of clinical microbiology. 7th ed., Washington DC, p. 1526–1543.
Leite de Andrade MC, Soares de Oliveira MA, Santos FAGD, Ximenes Vilela PB, da Silva MN, Macêdo DPC, de Lima Neto RG, Neves HJP, Brandão ISL, Chaves GM, de Araujo RE, Neves RP (2017) A new approach by optical coherence tomography for elucidating biofilm formation by emergent Candida species. PLoS One 12(11): e0188020.
Leonardi D, Barrera MG, Lamas MC, Salomon CJ (2007) Development of prednisone: polyethylene glycol 6000 fast-release tablets from solid dispersions: solid-state characterization, dissolution behavior, and formulation parameters. AAPS PharmSciTech 8(4): E108
Leonardi D, Salomon CJ (2013) Unexpected performance of physical mixtures over solid dispersions on the dissolution behavior of benznidazole from tablets. J Pharm Sci 102: 1016-1023.
Li J, Barrow D, Howell H, Kalachandra S (2010) *In vitro* drug release study of methacrylate polymer blend system: effect of polymer blend composition, drug loading and solubilizing surfactants on drug release. J Mater Sci Mater Med 21: 583-588.
López-Sánchez A, Pérez-Cantero A, Torrado-Salmerón C, Martin-Vicente A, García-Herrero V, González-Nicolás MÁ, Lázaro A, Tejedor A, Torrado-Santiago S, García-Rodríguez JJ, Capilla J, Torrado S (2018) Efficacy, biodistribution, and nephrotoxicity of experimental Amphotericin B-Deoxycholate formulations for pulmonary aspergillosis. Antimicrob Agents Chemother 62: pii: e00489-18.
Maki DG, Weise CE, Sarafin HW (1977) A semiquantitative culture method for identifying intravenous catheter related infection. N Engl J Med 296: 1305–1309.
Marcos-Zambrano LJ, Puig-Asensio M, Pérez-García F, Escribano P, Sánchez-Carrillo C, Zaragoza O, Padilla B, Cuenca-Estrella M, Almirante B, Martín-Gómez MT, Muñoz P, Bouza E, Guinea J (2017) *Candida guilliermondii* complex is characterized by high antifungal resistance but low mortality in 22 cases of candidemia. J. Antimicrob Agents Chemother 61: pii: e00099-17.
Martín-Rabadán P, Pérez-García F, Zamora Flores E, Nisa ES, Guembe M, Bouza E (2017) Improved method for the detection of catheter colonization and catheter-related bacteremia in newborns. Diagn Microbiol Infect Dis 87: 311-314.
Mayer FL, Wilson D, Hube B (2013) *Candida albicans* pathogenicity mechanisms. Virulence 4: 119-128.
Melkusová S, Bujdáková H, Volleková A, Myoken Y, Mikami Y (2004) The efficiency of the benzothiazole APB, the echinocandin micafungin, and amphotericin B in fluconazole-resistant *Candida albicans* and *Candida dubliniensis*. Pharmazie 59: 573-574.
Ng KP, Kuan CS, Kaur H, Na SL, Atiya N, Velayuthan RD (2015) *Candida* species epidemiology 2000-2013: a laboratory-based report. Trop Med Int Health 20: 1447-1453.
Palmeiro-Roldán R, Fonseca-Berzal C, Gómez-Barrio A, Arán VJ, Escario JA, Torrado-Durán S, Torrad-Santiago S (2014) Development of novel benznidazole formulations: Physicochemical characterization and in vivo evaluation on parasitemia reduction in Chagas disease. Int J Pharm 472: 110-117.
Paredes K, Pastor FJ, Capilla J, Sutton DA, Mayayo E, Fothergill AW, Guarro J (2015) Therapies against murine *Candida guilliermondii* infection, relationship between in vitro antifungal pharmacodynamics and outcome. Rev Iberoam Micol 32: 34-39.
Park JB, Prodduturi S, Morott J, Kulkarni VI, Jacob MR, Khan SI, Stodghill SP, Repka MA (2015) Development of an antifungal denture adhesive film for oral candidiasis utilizing hot melt extrusion technology. Expert Opin Drug Deliv 12: 1-13.
Rangel-Yagui CO, Pessoa A Jr, Tavares LC (2005) Micellar Solubilization of drugs. J Pharm Pharm Sci 8: 147–163.
Talukder R, Reed C, Dürig T, Hussain M (2011) Dissolution and solid-state characterization of poorly water-soluble drugs in the presence of a hydrophilic carrier. AAPS PharmSciTech 12: 1227-1233.
Tambunlertchai S, Srisang S, Nasongkla N (2017) Development of antimicrobial coating by later-by-layer dip coating of chlorhexidine-loaded micelles. J Mater Sci Mater Med 28: 90.
Tobudic S, Kratzer C, Lassnigg A, Presterl E (2012) Antifungal susceptibility of *Candida albicans* in biofilms. Mycoses 55: 199-204.
Uppuluri P, Dinakaran H, Thomas DP, Chaturvedi AK, Lopez-Ribot JL (2009) Characteristics of *Candida albicans* biofilms grown in a synthetic urine medium. J Clin Microbiol 47: 4078–4083.
Vadlapatla R, Fifer EK, Kim CJ, Alexander KS (2009) Drug-organic electrolyte complexes as controlled release systems. Drug Dev Ind Pharm 35: 1-11.
Vippagunta SR, Maul KA, Tallavajhala S, Grant DJ (2002) Solid-state characterization of nifedipine solid dispersions. Int J Pharm 236: 111-123.
Yuan X, Wang R, Bai CQ, Song XJ, Liu YN (2012) Caspofungin for prophylaxis and treatment of fungal infections in adolescents and adults: a meta-analysis of randomized controlled trials. Pharmazie 67: 267-73.